Supporting Information

Boron nanosheet as a phosphatase mimicking nanozyme with ultrahigh catalytic activity for prodrug-based cancer therapy

Yao Lei,[‡a] Qianghong Zhao,[‡a] Zhou Huang, [b] Yusha Huang, [a] Min Wang,*[a] Lianzhe Hu,*[c] Qing Tang,*[b] and Zhining Xia [a]

[a.] Chongqing Key Laboratory of Natural Product Synthesis and Drug Research, Innovative Drug Research Center, School of Pharmaceutical Sciences, Chongqing University Chongqing 401331, China.

[b.] School of Chemistry and Chemical Engineering, Chongqing Key Laboratory of Theoretical and Computational Chemistry, Chongqing University, Chongqing 401331, China.

[c.] Chongqing Key Laboratory of Green Synthesis and Applications, College of Chemistry, Chongqing Normal University, Chongqing, 401331, China.

* Corresponding author. E-mail: wang_min@cqu.edu.cn; lianzhehu@cqnu.edu.cn; qingtang@cqu.edu.cn

‡ These authors contributed equally to this work.

Experimental Section

Reagents and materials

Boron powder, 4-methylumbelliferyl phosphate (4-MUP) disodium salt, 4-methylumbelliferone (4-MU), ethylene glycol, glycerol, ethylenediamine, glucose, D-(+)-mannose, N-methylacridone (NMA), tris(penta-fluorophenyl)-borane (BCF), amine functionalized polyethylene glycol (PEG-NH_2, 2 kDa), and 3-[4,5-dimethylthiazol-2-yl]-2,5-diphenyl tetrazolium bromide (MTT) were supplied by Aladdin Biological Technology Co., Ltd. (Shanghai, China). ZrO_2 nanoparticle was purchased from XFNano Materials Tech Co., Ltd (Nanjing China). N-methyl-2-pyrrolidone (NMP), anhydrous ethanol, dimethyl sulfoxide (DMSO), sodium borohydride ($NaBH_4$), sodium tetraborate decahydrate ($Na_2B_4O_7 \cdot 10H_2O$), diboron trioxide (B_2O_3) and boric acid (H_3BO_3) were provided by Chengdu Kelong Chemical Co., Ltd. (Sichuan, China). 4-nitrophenyl phosphate (*p*-NPP) disodium salt hexahydrate was purchased from Meryer Biochemical Technology Co., Ltd. (Shanghai, China). 4-nitrophenyl acetate (*p*-NPA) and 4-nitrophenyl sulfate (*p*-NPS) potassium salt were obtained from Sigma-Aldrich (St. Louis, MO, USA). 4-(2-hydroxyethyl)-1-piperazineethanesulfonic acid (HEPES) was purchased from Shanghai Titan Technology Co., Ltd. (Shanghai, China). Combretastatin A4 disodium phosphate (CA4P) was provided by Nantong Feiyu Biotechnology Co., Ltd. (Jiangsu, China). Annexin V-FITC apoptosis detection kit was purchased from Beyotime Biotechnology (Shanghai, China). Dulbecco's modified eagle medium (DMEM) with high glucose, fetal bovine serum (FBS) and penicillin-streptomycin were bought from Gibco Life Technologies (USA). Trypsin was obtained from Guangzhou Sopo Biological Technology Co., LTD. (Guangdong, China).

Characterization

The fluorescence spectra were measured on an F-4600 fluorescent spectrophotometer (Shimadzu, Japan). The UV-vis absorption spectra were acquired on a Cary60 spectrophotometer (Agilent, USA). Transmission electron microscopy (TEM) images were collected on a Talos F200S transmission electron microscope

(Thermo Fisher Scientific, USA). Zeta potential data were collected on a Nanobrook Omni zeta potential analyzer (Brookhaven, USA). X-ray photoelectron spectroscopy (XPS) measurements were performed on an ESCALAB 250Xi spectrometer (Thermo Fisher Scientific, USA). Atomic force microscopy (AFM) images were collected on a MFP-3D-BIO atomic force microscope (Asylum Research, USA). High-performance liquid chromatography (HPLC) analysis was achieved on LC-20A system (Shimadzu, Japan). Analysis of 96-well microplates were performed on a SpectraMax i3x reader (Molecular Devices, USA). Flow cytometry data were acquired on a FACSAria II cell sorter (Becton Dickinson, USA).

Preparation of BNS and PEG-NH_2 functionalized BNS (PEG@BNS)

BNS was prepared through a liquid exfoliation approach with the assistance of thermal oxidation etching according to the previous report.[1] Briefly, 5 g/mL boron powder in ethanol-NMP (1:1 v/v) was probe sonicated for 16 h in ice-bath at 500 W. The boron chunks in the solution were removed by the centrifugation at 3000 rpm for 10 min. Then the supernatant underwent centrifugation at 12000 rpm for 20 min, washing with ethanol for 3 time and drying at 30 ^{o}C overnight. The black boron powder after the first liquid exfoliation was obtained and named as boron sheet.

For the thermal oxidation etching, the above boron sheets were laid on the surface of the crucible, followed by heating at 650 ^{o}C for 2 h. After cooling, the obtained brown powder (named as oxidized boron sheet) was dispersed in water for the second probe sonication. After centrifugation at 12000 rpm and drying at 30 ^{o}C, BNS was collected and dispersed in 20 mM HEPES buffer (pH 8.5) for further use.

For the preparation of PEG@BNS, 10 mg PEG-NH_2 was added into 200 μg/mL BNS aqueous solution and stirred for 12 h. After removing the unmodified PEG-NH_2 by the dialysis, the solution was centrifuged at 2500 rpm for 30 min and washed with water for 3 times. The collected PEG@BNS was dispersed in water for further use.

For the activity comparison, CeO_2 nanoparticle and Uio-66 were prepared according to exactly the same methods in the previous reports.[2, 3]

The phosphatase-like catalytic activity of BNS

4-MUP and *p*-NPP were employed as the model substrates for evaluating the

phosphatase-like catalytic activity of BNS. The time-dependent responses of 25 μg/mL BNS in 20 mM HEPES buffer solution (pH 8.5) containing 5 μM 4-MUP or 500 μM *p*-NPP were monitored. For fluorescence response, the fluorescence intensity at 448 nm was monitored for 10 min under excitation at 360 nm. For UV-vis absorption response, the absorbance at 405 nm was monitored for 20 min.

For the phosphatase-like activity comparison of BNS with the reported phosphatase-like nanozymes, the phosphatase-like activities of CeO_2 NPs, ZrO_2 NPs and Uio-66 at the same mass concentration (25 μg/mL) were tested by using 4-MUP as the substrate. To investigate the effect of solution pH, BNS and ALP were incubated at different pH values (i.e. 2.5, 4.0, 5.5, 7.0, 8.5 and 10.0) for 2 h, and then the activities were analyzed at pH 8.5. To test the thermal stability of BNS and ALP, BNS and ALP were incubated in 20 mM HEPES buffer (pH 8.5) at different temperatures (i.e. 15, 30, 45 and 60 ^oC) for 2 h, and then the activities were analyzed at room temperature.

Quantification of Lewis acidity by NMA probe

BNS suspension (4 mg/mL in acetonitrile) and NMA solution (20 μM in acetonitrile) were degassed with N_2 for 20 min and then mixed together in a 1:1 volume ratio. The resulting mixture was sonicated for 10 min. The fluorescence emission spectra were measured under excitation at 360 nm. For a positive control, the Lewis acidity of the boron-based Lewis acid BCF was also tested by using the same procedure.

Catalytic conversion of CA4P by PEG@BNS

50 μL of CA4P (100 μg/mL) was mixed with 450 μL of PEG@BNS dispersion in phosphate buffer solution (PBS, pH 7.4). After incubation at 37 ^oC for 0.5 h, the supernatant was collected by filtration and analyzed by HPLC on a C18 column with acetonitrile and water (containing 0.4% formic acid) (1:1 v/v) as the mobile phase. The detection wavelength was 295 nm.

Cell viability assay and flow cytometry analysis

For cell culture, HeLa cells cultured in DMEM supplemented with 10% FBS and 1% penicillin-streptomycin in 100% humidified atmosphere containing 5% CO_2 at 37 ^oC.

To evaluate the cytotoxicity of PEG@BNS, HeLa cells were seeded onto 96-well plates, and cultured at 37 ^{o}C for 24 h. Then the cells were incubated with PEG@BNS at different concentrations (i.e. 0, 10, 25, 50, 80, 100 and 200 μg/mL) for 24 h and washed with PBS. 100 μL of MTT solution was added into each well and the cells were cultured for 4 h. After removing the supernatant, 150 μL of DMSO was added into each well to dissolve the formazan crystals. Finally, the absorbance at 490 nm was recorded on a SpectraMax i3x reader.

To test the cell inhibition of CA4P with the assistance of PEG@BNS, HeLa cells on 96-well plates were pretreated with 25 μg/mL PEG@BNS for 6 h. After wash with PBS, the cells were incubated with CA4P at different concentrations (i.e. 0, 0.01, 0.1, 1, 2, 5 and 8 μg/mL) for 24 h, followed by MTT testing described in the cytotoxicity evaluation. As a control, the cell inhibition of CA4P was also tested by using the untreated cells.

Then the intracellular CA4P conversion catalyzed by PEG@BNS was further tested by flow cytometry analysis. Briefly, HeLa cells were seeded onto six-well plates and cultured at 37 ^{o}C for 24 h. Then the cells were treated with 25 μg/mL PEG@BNS. After wash with PBS, the treated cells were incubated with 3.2 μg/mL CA4P for 24 h. Finally, the cells were collected through the trypsin treatment, washed with PBS, and labelled with Annexin V-FITC apoptosis detection kit for flow cytometry analysis.

Computational methods and models

All DFT calculations were performed using the Vienna Ab initio Simulation Package (VASP 5.4.4).[4] The Perdew-Burke-Ernzerhof (PBE) functional[5] were employed to calculate the exchange-correlation energy, where the Grimme's D3 dispersion[6] was involved. The plane wave basis sets with an energy cutoff of 400 eV were used for valence electrons, and the projector-augmented-wave (PAW) pseudopotentials[7, 8] were employed for core electrons. Structural relaxation was performed using a conjugated-gradient algorithm with the convergence criteria of 10^{-5} eV and 0.02 eV Å^{-1} in energy and force, respectively. Transition states were located using the "climbing images" nudged elastic band (CI-NEB)[9] and dimer methods with the same convergence criteria as that for geometry optimization. For BNS, a vacuum

separation of 15 Å along the *z*-direction was set between two periodically repeated slabs, and a cubic lattice of 20 Å was used for the calculations of small molecules and groups. The Monkhorst-Pack-grid-mesh-based Brillouin zone k-points are set as 2×2×1 for all periodic structure. The frequencies of relevant structures were analyzed to obtain their Gibbs free energies.

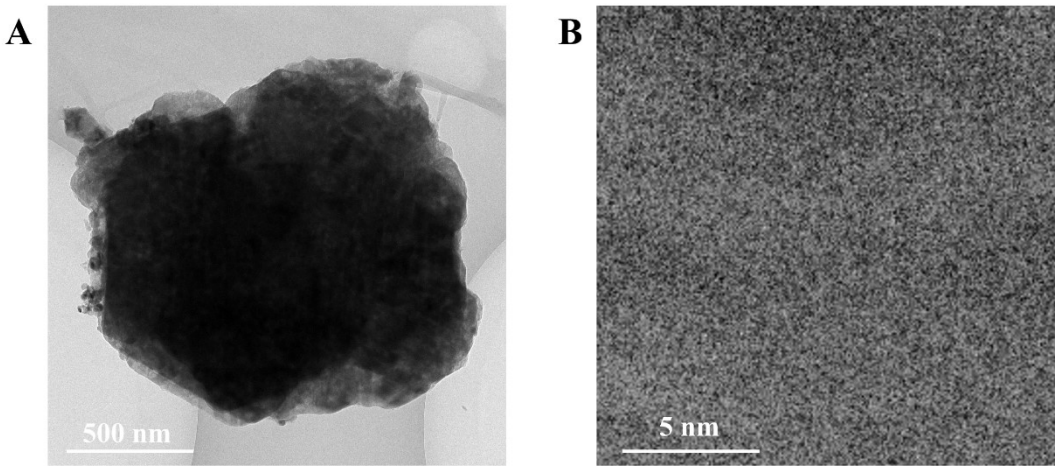

Fig. S1 TEM (A) and HRTEM (B) images of the raw material boron powder.

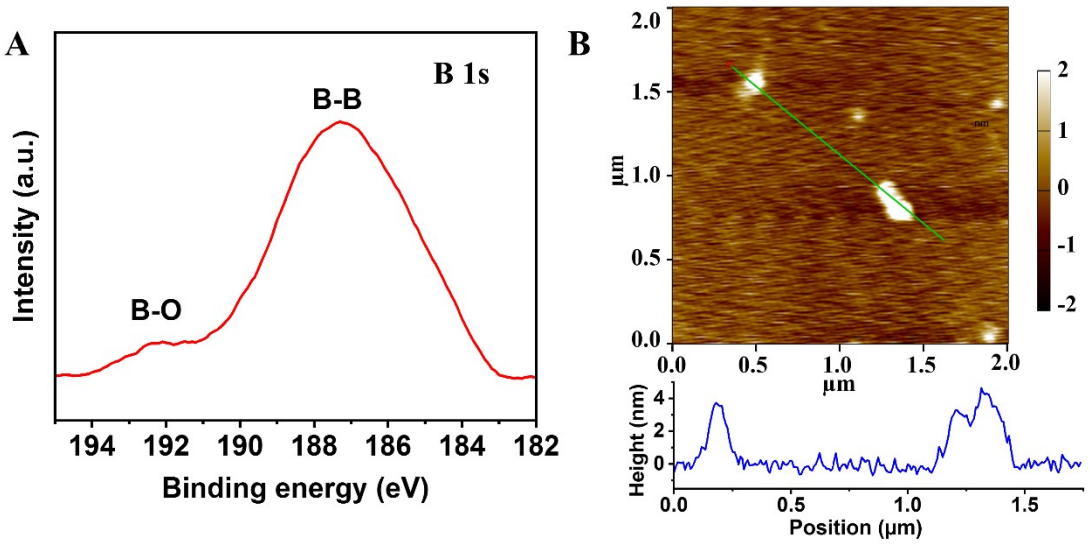

Fig. S2 (A) B 1s XPS spectrum of BNS. (B) Representative AFM topographic image and the corresponding height profile of BNS.

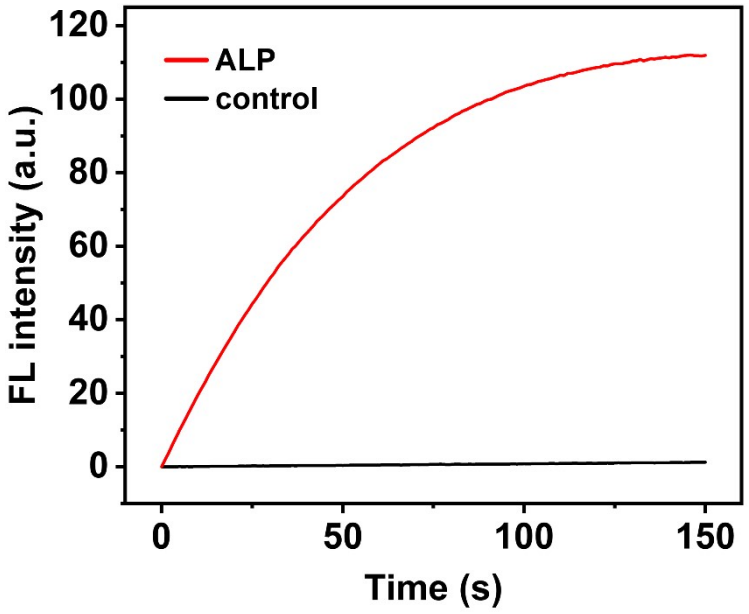

Fig. S3 Kinetic curves of 5 μM 4-MUP (control), and 5 μM 4-MUP in the presence of ALP.

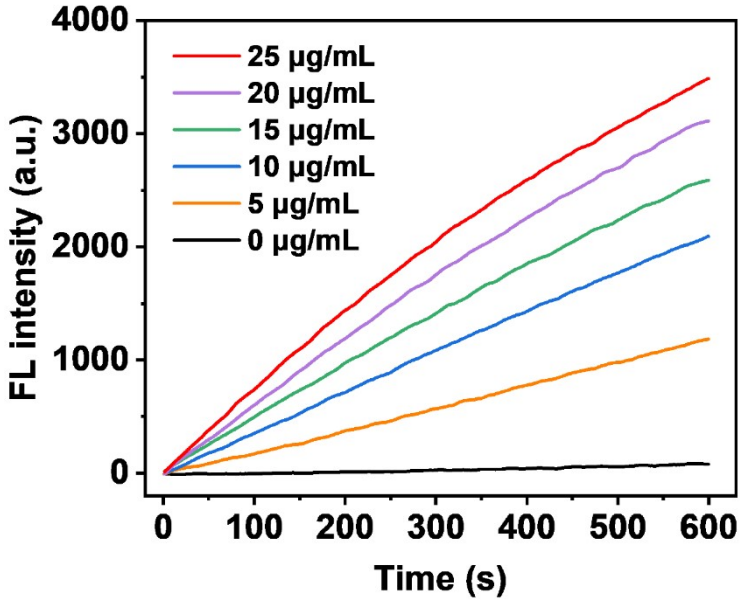

Fig. S4 Kinetic curves of 5 μM 4-MUP in the presence of different concentrations of BNS (i.e. 0, 5, 10, 15, 20 and 25 μg/mL).

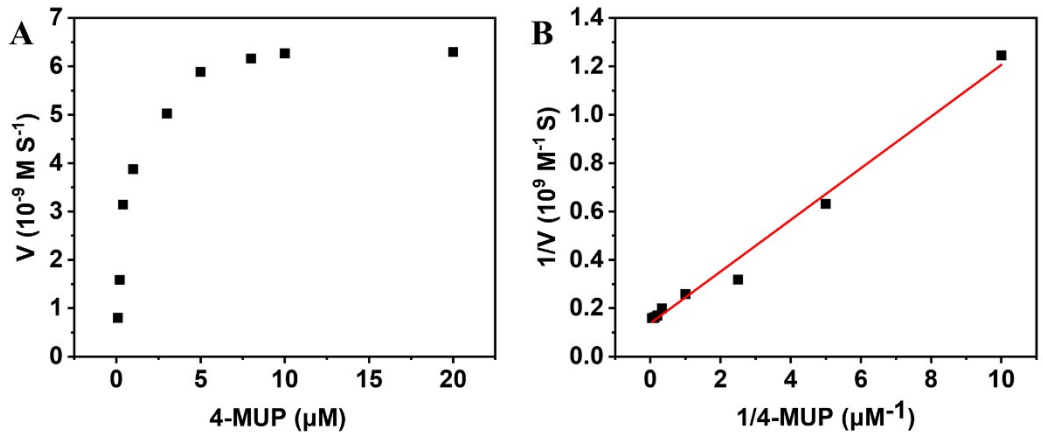

Fig. S5 (A) Steady-state kinetic assay of BNS by varying concentration of 4-MUP (i.e., 0.1, 0.2, 0.4, 1, 3, 5, 8, 10 and 20 μM). (B) Lineweaver-Burk plot of BNS obtained from Fig. S3A according to the double reciprocal of the Michaelis-Menten equations.

Table S1 Comparison of the apparent K_m of BNS nanozyme with that of ALP and the reported phosphatase-like nanozymes.

Catalyst	Substrate	K_m / μM	Reference
CeO_2 NPs	4-MUP	16.5	[10]
ZrO_2 NPs	4-MUP	14.7	[10]
Uio-66	4-MUP	7.0	This work
BNS	4-MUP	0.78	This work
ALP	4-MUP	1.13	[10]

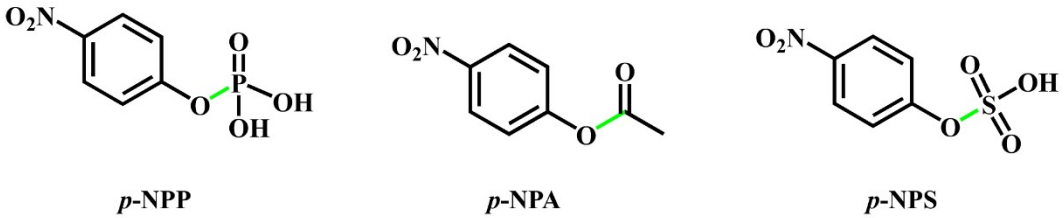

Fig. S6 Structural formulas of three chromogenic substrates *p*-NPP, *p*-NPA and *p*-NPS.

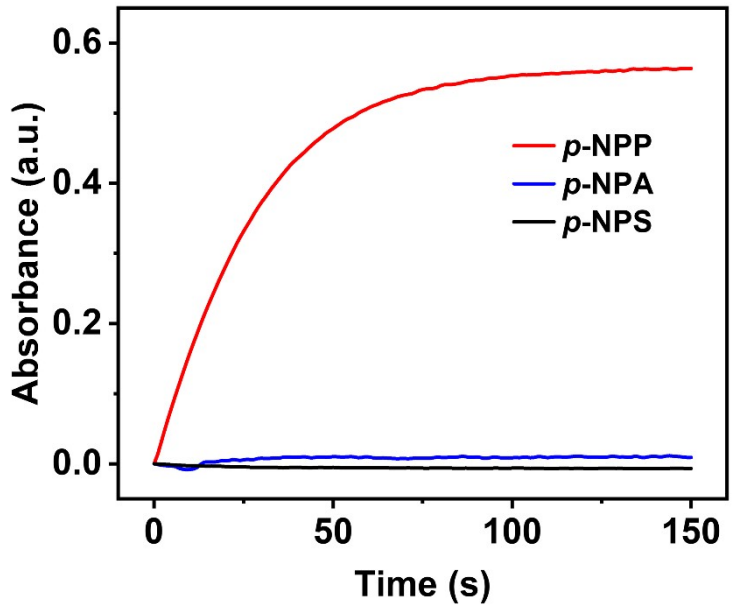

Fig. S7 Kinetic curves of 500 μM *p*-NPA (a), *p*-NPS (b) and *p*-NPP (c) in the presence of natural phosphatase (i.e., ALP).

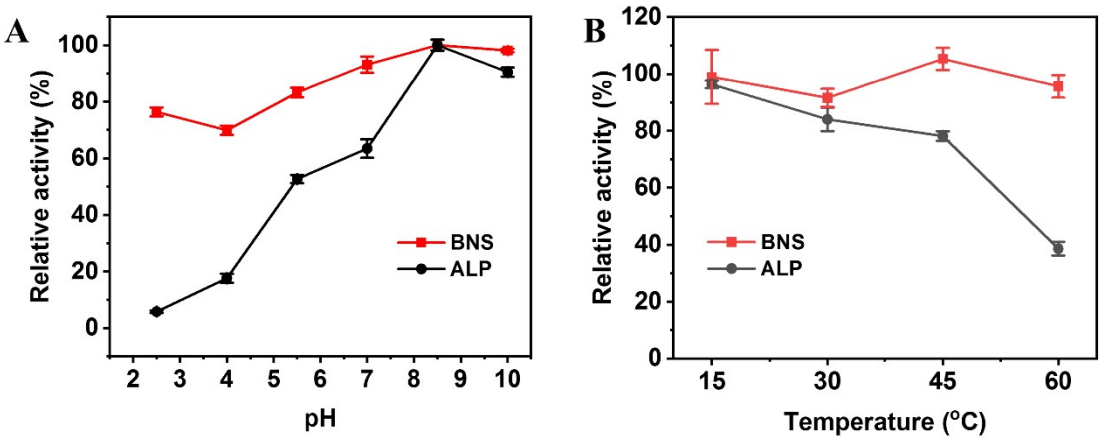

Fig. S8 The effect of pH (A) and temperature (B) on the stability of catalytic activities of BNS and ALP.

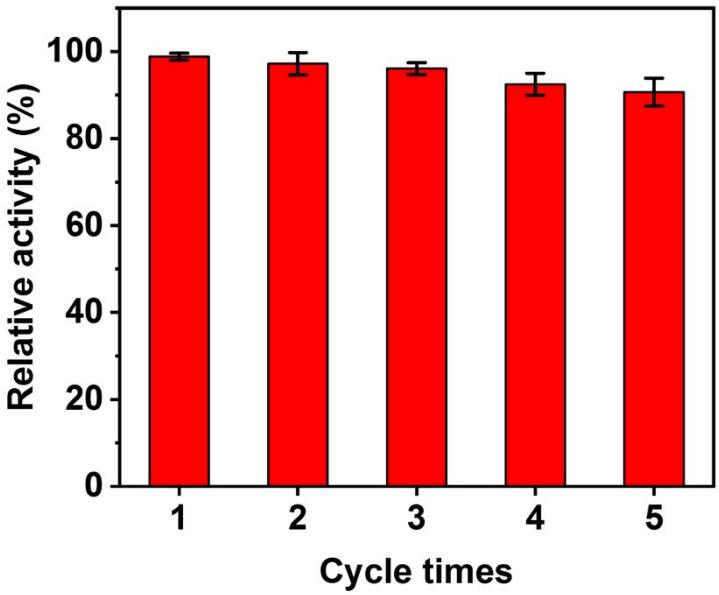

Fig. S9 Cycling runs of hydrolysis of 4-MUP in the presence of BNS.

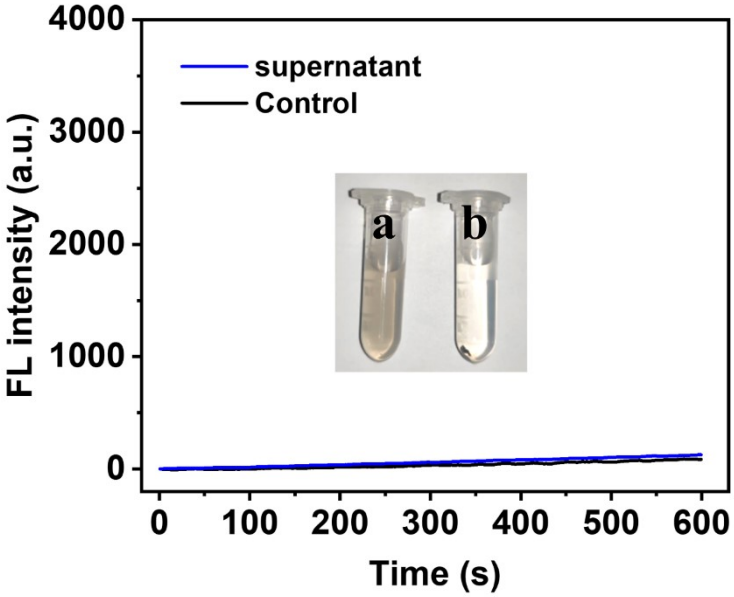

Fig. S10 Kinetic curves of 5 μM 4-MUP in the absence and presence of the supernatant of 25 μg/mL BNS. Inset: the photo of the BNS dispersion before and after centrifugation.

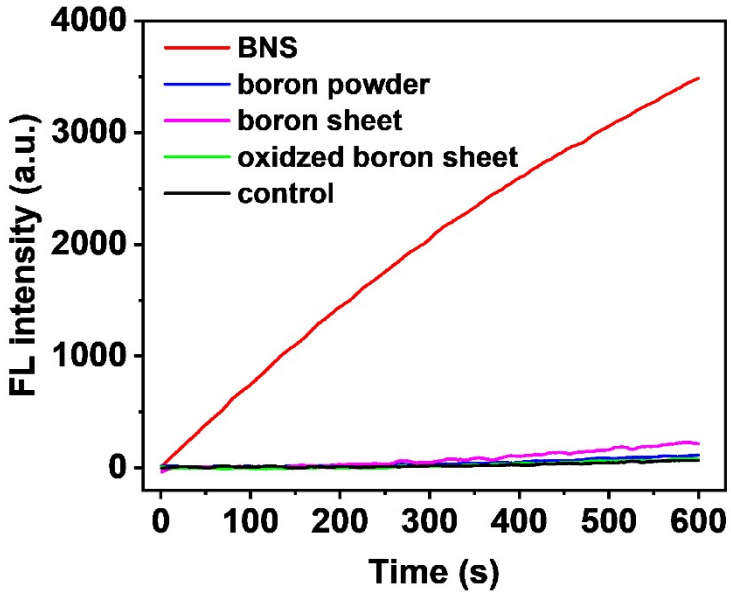

Fig. S11 Kinetic curves of 5 μM 4-MUP (control), and 5 μM 4-MUP in the presence of the raw material (i.e., boron powder), two intermediate materials (i.e., boron sheet prepared from the first liquid exfoliation of boron powder and oxidized boron sheet prepared from thermal oxidation of boron sheet), or BNS.

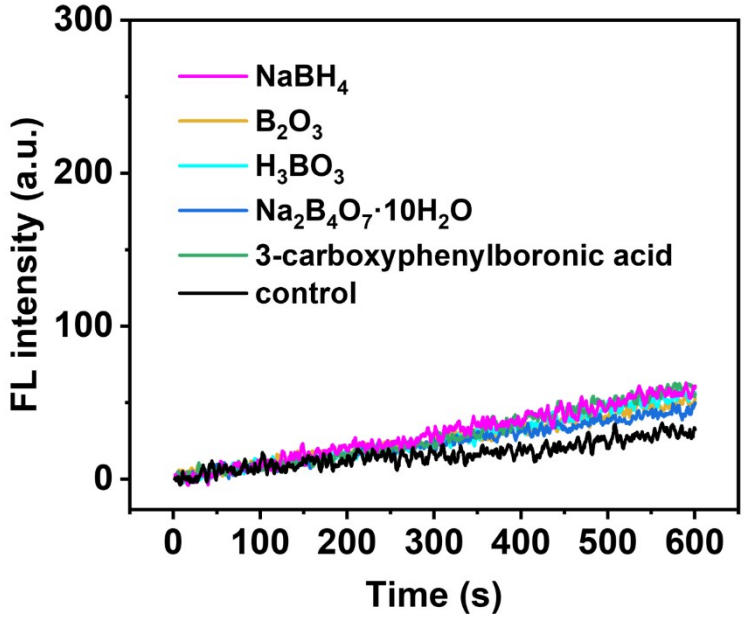

Fig. S12 Kinetic curves of 5 μM 4-MUP (control), and 5 μM 4-MUP in the presence of different boron-based compounds.

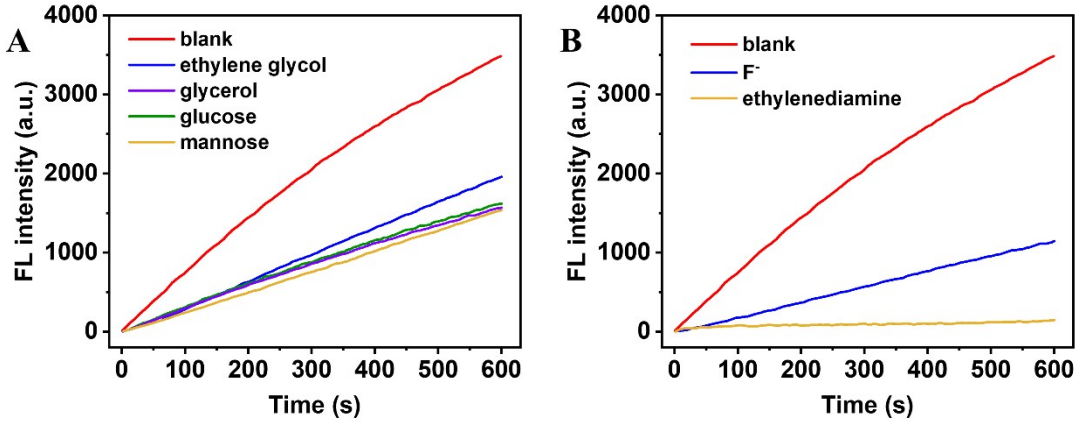

Fig. S13 (A) Kinetic curves of the mixture of 5 μM 4-MUP and 25 μg/mL BNS in the absence (blank) and presence of 5% (v/v) ethylene glycol, 5% (v/v) glycerol, 5 mM glucose or 5 mM mannose. (B) Kinetic curves of the mixture of 5 μM 4-MUP and 25 μg/mL BNS in the absence (blank) and presence of 5 mM F^- or 5% (v/v) ethylenediamine.

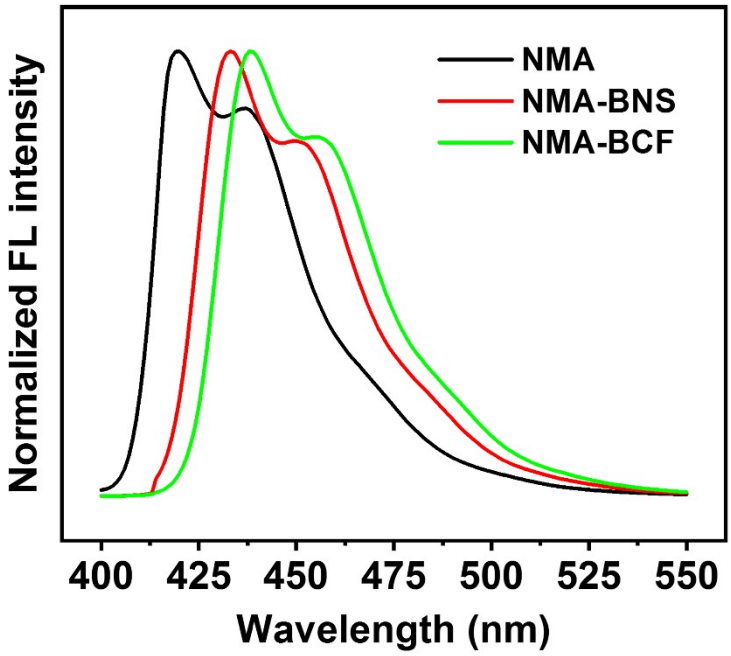

Fig. S14 Fluorescence spectra of NMA, NMA-BNS and NMA-BCF.

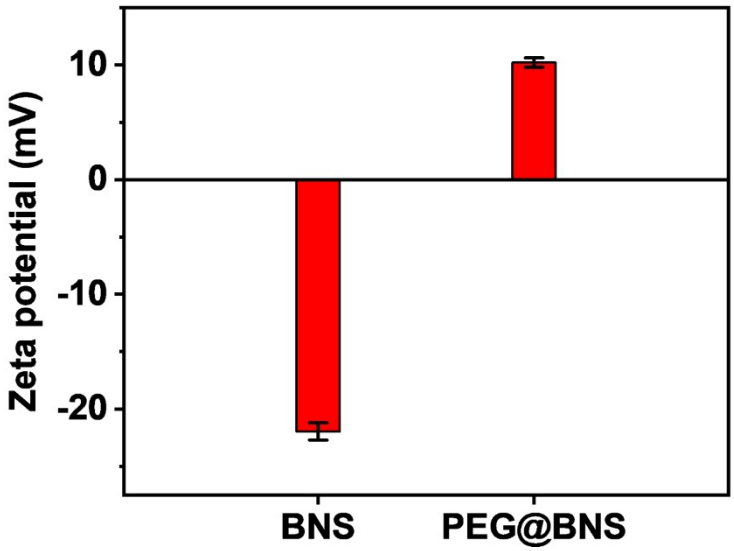

Fig. S15 Zeta potential of BNS and PEG@BNS.

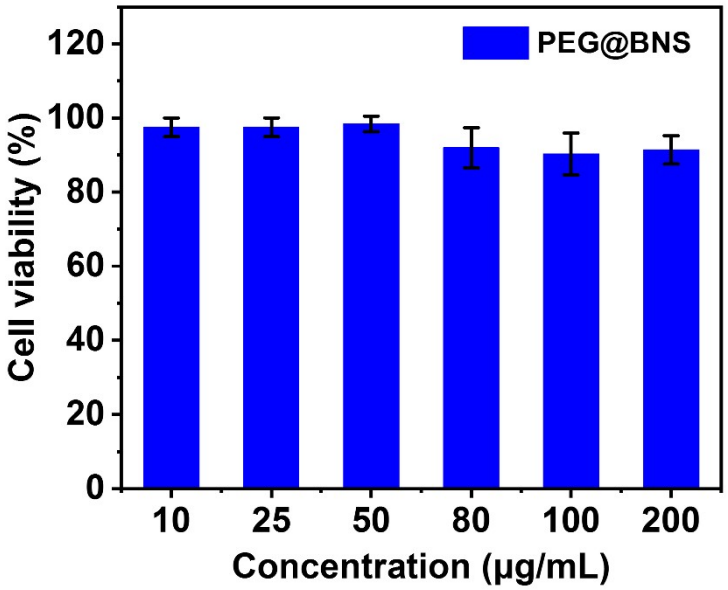

Fig. S16 Viability of HeLa cells after incubation with different concentrations of PEG@BNS for 24 h.

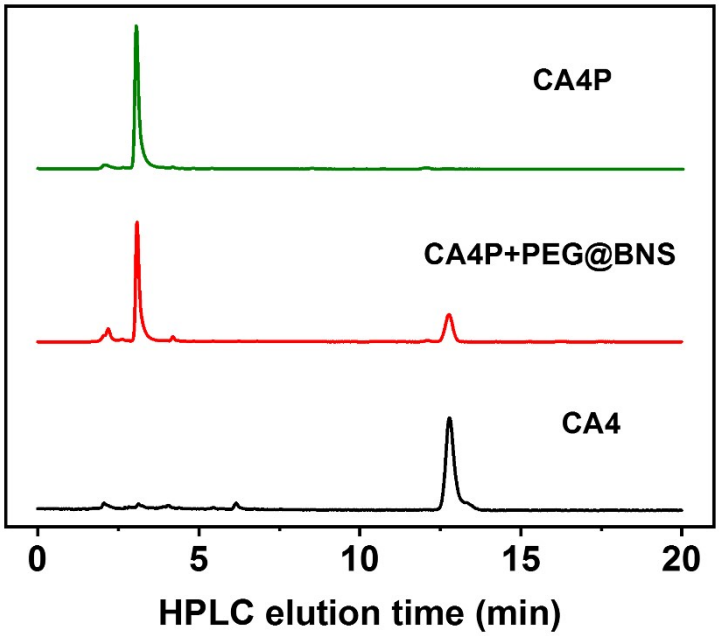

Fig. S17 HPLC chromatogram of CA4P, CA4, and CA4P after incubation with PEG@BNS for 30 min.

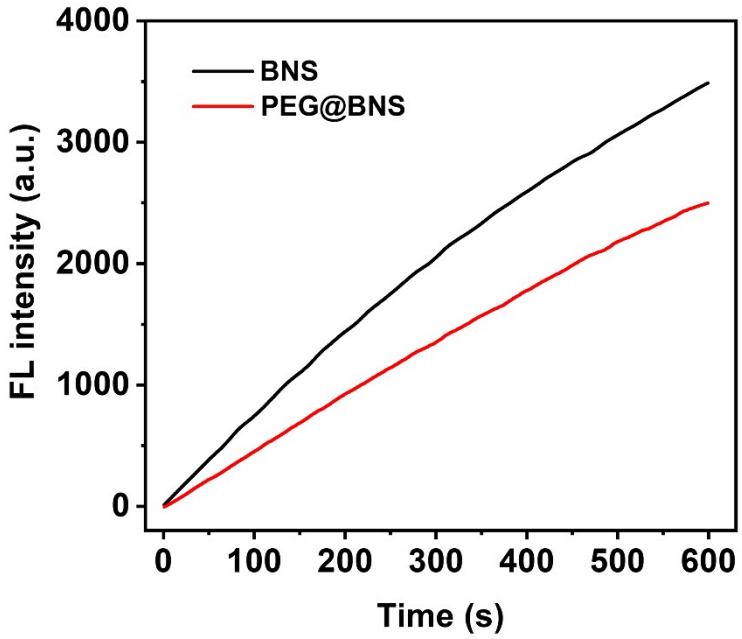

Fig. S18 Kinetic curves of 5 μM 4-MUP in the presence of 25 μg/mL BNS or PEG@BNS.

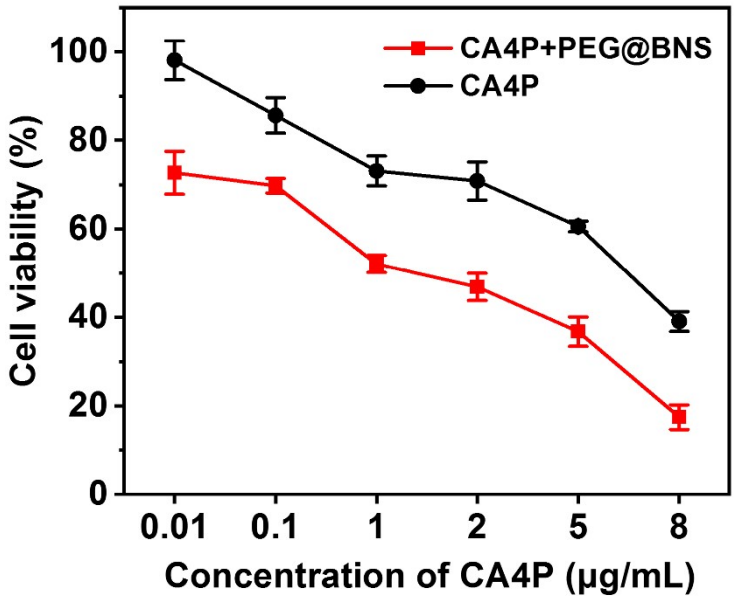

Fig. S19 Effects of different concentrations of CA4P on the viability of HeLa cells with and without PEG@BNS pretreatment.

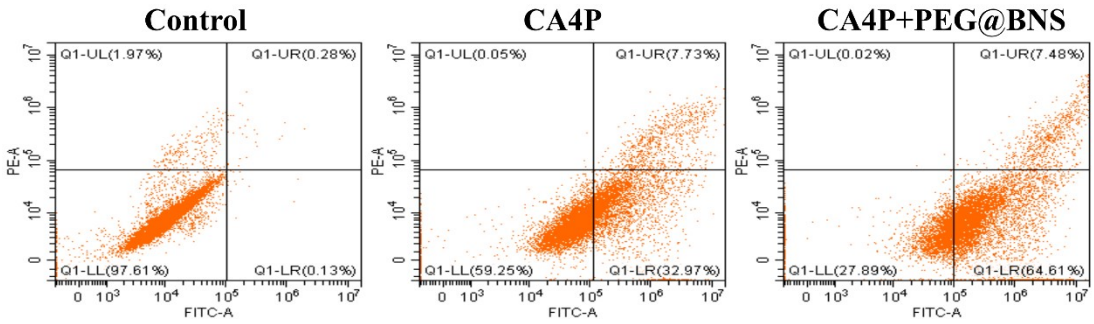

Fig. S20 Flow cytometry data of untreated HeLa cells (control), HeLa cells treated with CA4P, and HeLa cells treated with CA4P after PEG@BNS pretreatment.

Reference

1. X. Ji, N. Kong, J. Wang, W. Li, Y. Xiao, S. T. Gan, Y. Zhang, Y. Li, X. Song, Q. Xiong, S. Shi, Z. Li, W. Tao, H. Zhang, L. Mei and J. Shi, *Adv. Mater.*, 2018, **30**, 1803031.
2. X. Tian, H. Liao, M. Wang, L. Feng, W. Fu and L. Hu, *Biosens. Bioelectron.*, 2020, **152**, 112027.
3. M. Xu, L. Feng, L.-N. Yan, S.-S. Meng, S. Yuan, M.-J. He, H. Liang, X.-Y. Chen, H.-Y. Wei, Z.-Y. Gu and H.-C. Zhou, *Nanoscale*, 2019, **11**, 11270-11278.
4. G. Kresse and J. Furthmuller, *Phys. Rev. B*, 1996, **54**, 11169-11186.
5. J. P. Perdew, K. Burke and M. Ernzerhof, *Phys. Rev. Lett.*, 1996, **77**, 3865.
6. S. Grimme, *J. Comput. Chem.*, 2006, **27**, 1787-1799.
7. P. E. Blochl, *Phys. Rev. B*, 1994, **50**, 17953-17979.
8. G. Kresse and D. Joubert, *Phys. Rev. B*, 1999, **59**, 1758-1775.
9. G. Henkelman, B. P. Uberuaga and H. Jónsson, *J. Chem. Phys.*, 2000, **113**, 9901-9904.
10. X. Hu, T. Huang, H. Liao, L. Hu and M. Wang, *J. Mater. Chem. B*, 2020, **8**, 4428-4433.